HCG MEMS tunable VCSEL with intracavity integrated detector

Carlos F. Mateus, Dalila Ellafi, Chuanshun Cao, Virgil Carl Ford, Neelanjan Bandyopadhyay, et al.

Carlos F. R. Mateus, Dalila Ellafi, Chuanshun Cao, Virgil Carl Ford, Neelanjan Bandyopadhyay, Kai-C. A. Hui, Christopher Chase, D. Philip Worland, "HCG MEMS tunable VCSEL with intracavity integrated detector," Proc. SPIE 12439, Vertical-Cavity Surface-Emitting Lasers XXVII, 1243906 (15 March 2023); doi: 10.1117/12.2668721

Event: SPIE OPTO, 2023, San Francisco, California, United States

HCG MEMS tunable VCSEL with intracavity integrated detector

Carlos F. R. Mateus*, Dalila Ellafi, Chuanshun Cao, Virgil Carl Ford, Neelanjan Bandyopadhyay, Kai-C A. Hui, Christopher Chase, D. Philip Worland
Bandwidth10, Inc. - 2080 Addison St., Berkeley, CA, USA - 94704

ABSTRACT

We report the design and manufacturing of a tunable VCSEL with an HCG MEMS mirror and an integrated detector oblique to the optical cavity for measuring output power without disturbing the laser cavity. This allows for a single laser device with integrated power monitoring capabilities that can be used in concert with external electronics to stabilize the power or monitor optical feedback of the device for sensing applications. The HCG tunable VCSEL is modified to incorporate a sacrificial layer capable of detecting light at the VCSEL's operating wavelength. For the MEMS release process, the sacrificial layer is removed from the optical cavity defined by the VCSEL mirrors and active region. The release process is designed to create a cavern around the optical cavity and walls of such cavern are composed by sacrificial layer material. Thus, the sacrificial layer material is removed from the optical cavity, but is kept surrounding it. Light scattered at the interface semiconductor-air hits the cavern walls and modifies current through the MEMS terminals (I_{det}). Any change in VCSEL output power (P_{out}) is directly related to a change on I_{det} through MEMS terminal, creating a direct relationship of P_{out} vs. I_{det}. To the best of our knowledge, there is no previous report of a VCSEL with integrated oblique intracavity detector.

Keywords: VCSEL, tunable VCSEL, tunable MEMS, detector, integrated detector.

1. INTRODUCTION

Monitoring of a VCSEL output optical power is required for many common and emerging applications of VCSELs such as optical communications, gas sensing, optical coherence tomography, LIDAR, and laser feedback interferometry. This is particularly true when a VCSEL is used as a prober for investigation of a particular phenomenon and power fluctuations of VCSEL can mask the effect under observation, cause saturation of detection or be directly used as a mechanism of sensing, as in the case for laser feedback interferometry [1].

External power monitoring schemes for VCSELs usually require bulky, costly, and complex optics and a beam splitter in the optical path for dropping a portion of power output or backside monitoring [2, 3]. An integrated detector provides the simplicity, compactness and robustness of a monolithic solution. Several proposals integrate a detector in the optical path [4 - 8], which has the downside of also possibly perturbating the cavity response due to feedback from the detector section, or require a complex scheme to couple light into detector region [2]. Our proposal uses only scattered light from inside the optical cavity, thus output power remains 100% integral and there is no extra loss for power monitoring.

2. DESCRIPTION OF DEVICE

Tunable VCSEL schemes with MEMS actuated mirror(s) have been extensively used [9]. Electrostatic actuation is the most used actuation mechanism, while several groups have also proposed piezoelectric [10] and thermal actuation [11]. For the electrostatic actuation, the MEMS mirror and the rest of VCSEL structure have to be electrically isolated in order to build charge in between the structures and allow electrostatic attraction. The insulating layer is also known as sacrificial layer, as it is partially removed under MEMS area in order to release the mirror structure and allow its movement. Usually, there is no sacrificial layer left in the optical path and sacrificial layer material is preserved only at the anchoring points.

Thus, the effort on design has always been in the direction of making the sacrificial layer as resistive as possible, for maximal electrical insulation. However, if the sacrificial layer material is correctly chosen to have its bandgap at the same wavelength of VCSEL operation and made slightly conductive (semi-insulating), then it is possible to consistently detect

*cmateus@bandwidth10.com; phone +1 (510) 990-8866; www.bandwidth10.com

Vertical-Cavity Surface-Emitting Lasers XXVII, edited by Chun Lei, Luke A. Graham,
Proc. of SPIE Vol. 12439, 1243906 · © 2023 SPIE
0277-786X · doi: 10.1117/12.2668721

light scattered from the cavity and monitor power levels of VCSEL, while still building charge for electrostatic actuation of MEMS HCG.

Fig. 1 shows a schematic of the HCG MEMS tunable VCSEL with oblique detector. Our current development is based on our standard tunable MEMS HCG VCSEL and details in VCSEL, HCG and MEMS design can be found elsewhere [12, 13]. The bottom portion of VCSEL is composed of ~30-40 pairs of DBR, active region, electrical aperture and spacing up to the sacrificial layer similar to as described in [12 -13]. Manufacturing and release of HCG mirror is through the small trenches around the HCG, so that the sacrificial layer is removed only from the optical cavity defined by the VCSEL mirrors and active region upon release. The release process is designed to create a cavern around the optical cavity, and walls of such cavern are composed of the sacrificial layer material. Thus, the sacrificial layer material is removed from the optical cavity itself, but is kept surrounding it. The overall fabrication and device performance are similar to that described in our previous works [12 -13].

The cavern walls senses light scattered at the interface semiconductor-air and transduction is further achieved as a change in electrical current through the MEMS terminals (I_{det}) relative to the dark current. Both the dark current and photocurrent are affected by the tuning voltage applied. Any change in VCSEL output power (P_{out}) directly affects I_{det} at the MEMS terminal, creating a direct relationship of P_{out} vs. I_{det}.

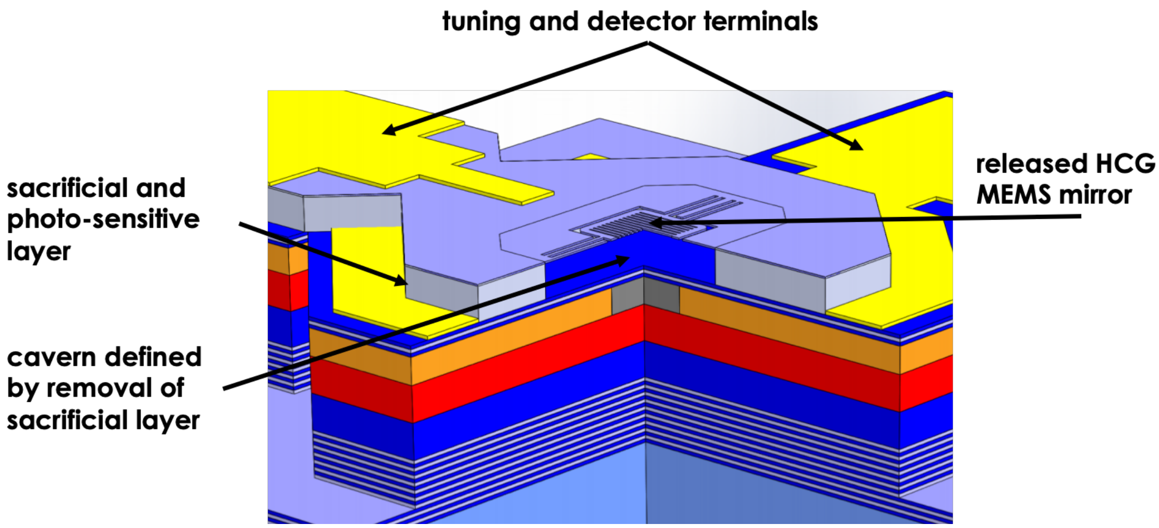

Figure 1. HCG MEMS tunable VCSEL with integrated tunable detector. The design of the MEMS release process forms a cavern around optical cavity defined by the HCG mirror and bottom DBR. Tuning (V_t) and detector (I_{det}) terminals are the same. The terminal touching the layer right below sacrificial layer is a common terminal for the laser. The second laser terminal is below bottom DBR and is not show in the schematic.

3. EXPERIMENTAL DATA

The following parameters are defined for the tunable HCG VCSEL:

I_{fwd} – VCSEL electrical pumping current, between the contact layer underneath the sacrificial layer and the bottom DBR;

I_{det} – detector electrical current, measured in between HCG layer and contact layer beneath the sacrificial layer (same terminals as V_t);

P_{out} – VCSEL output power as measured externally to the HCG;

V_t – tuning voltage, applied between the HCG layer and contact layer below the sacrificial layer to control lasing wavelength;

V_{fwd} – VCSEL voltage (voltage across laser), between the contact layer underneath the sacrificial layer and the bottom DBR.

Fig. 2(a) shows typical L-I (P_{out} vs. I_{fwd}) curves for a tunable VCSEL at different tuning voltages (V_t). Different wavelengths, given by different V_t, have different slope efficiency and threshold current. This is due to some design parameters, such as mirror design (both DBR and HCG), and spectral distribution of material gain, which cannot be made uniform over the full tuning range. Fig. 2 (b) shows I_{det} as function of I_{fwd}. I_{det} curve has a kink at laser threshold for each different wavelength and always change slope when VCSEL starts lasing. Fig. 3 shows a typical tuning spectrum for a tunable VCSEL at several different V_t. One can observe the designed transition between 2 longitudinal modes at ~6V and variation in power level over the tuning range.

Fig. 4 shows both P_{out} and I_{det} as function of I_{fwd} and in order to show the detail of I_{det} curve kink at threshold. The I_{det} curve has some dependence upon the I_{fwd} in addition to V_t. This dependence is likely to be related to the common contact serving both MEMS tuning and laser pump current, shown in Fig. 1. When I_{fwd} increases, V_{fwd} also increases and the total voltage across sacrificial layer increases from V_t, as a result. This may be removed by further optimization of design and fabrication process to better ground this contact. This dependence of I_{det} on I_{fwd} could also be removed via calibration in any real world application. In fact, most applications, such as swept-source for optical coherence tomography (OCT) or fiber Bragg grating sensing, consider an operation point at a fixed I_{fwd}.

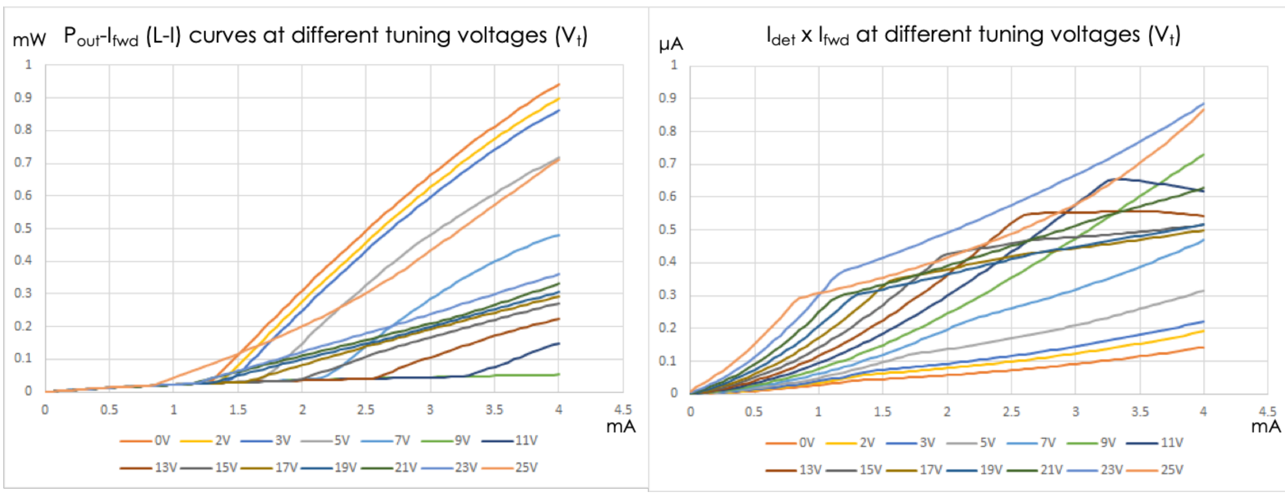

(a) (b)

Figure 2. Typical L-I curves for a tunable VCSEL and (b) I_{det} curve as function of I_{fwd} has a kink at laser threshold for each different wavelength and always change slope when VCSEL starts lasing.

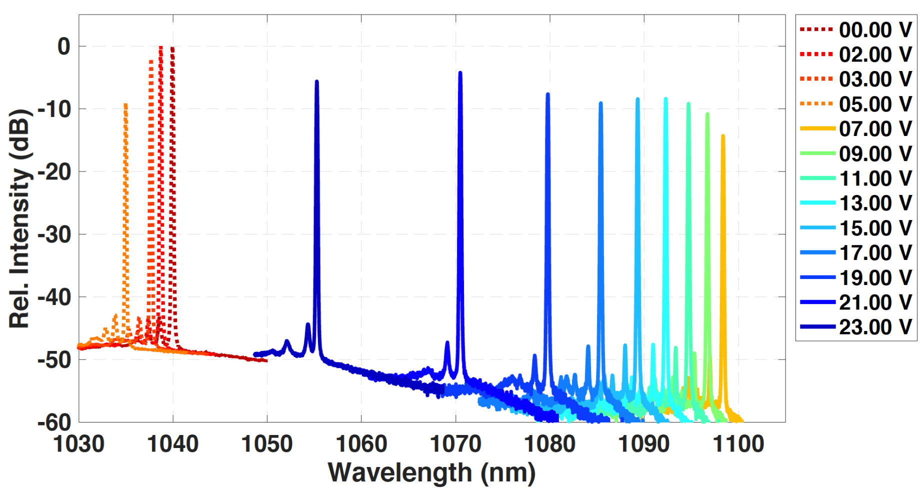

Figure 3. Typical tuning spectrum for a tunable VCSEL at several different Vt.

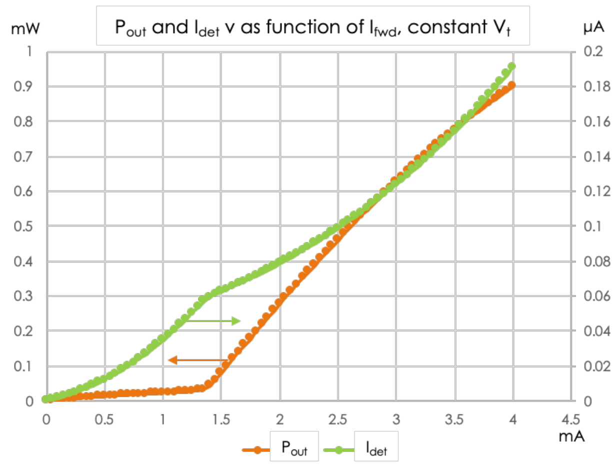

Figure 4. P_{out} and I_{det} curves as function of I_{fwd}, at constant V_t. I_{det} always change inclination and has a kink at laser threshold.

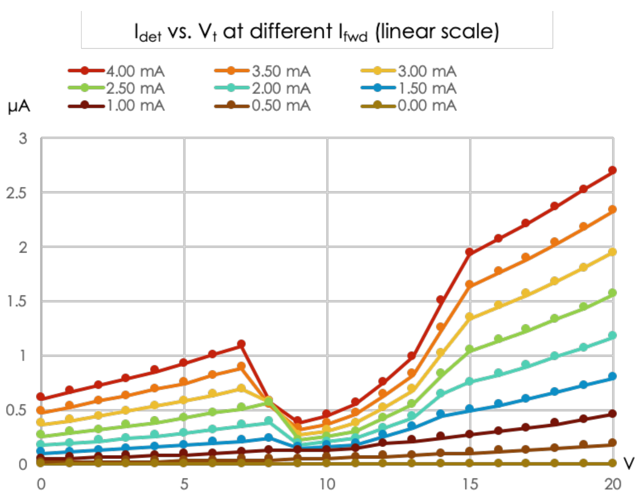

(a)

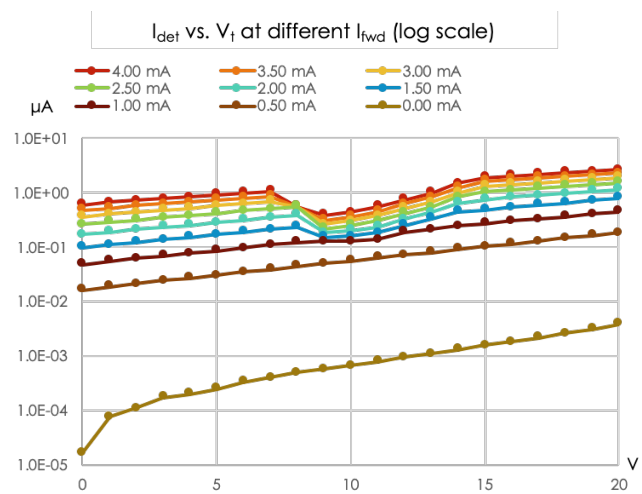

(b)

Figure 5. I_{det} vs. V_t ((a) linear scale and (b) log scale). When I_{fwd} <~1mA, there is no lasing and I_{det} vs. V_t is approximately linear on a logarithmic scale, as is expected for a reverse biased p-i-n junction. For I_{fwd} >1mA, VCSEL starts lasing and I_{det} follows laser power.

Fig. 5 was generated from a different device than in Figs. 2 to 4. Fig. 5 shows that VCSEL is not lasing at all different V_t, differently than previous figures. In other words, the VCSEL is only lasing within a limited spectral range. For example, at I_{fwd} = 4mA (see Fig. 5 (a), in blue) the VCSEL starts lasing at V_t = 7V and stops lasing above V_t = 15V. Note that in this case I_{det} vs. V_t is linear below 7V and above 15V. Fig. 5 (b) shows that I_{det} is negligible when I_{fwd} is zero, in fact 100x smaller than I_{fwd} = 0.5mA. If we look at a specific tuning voltage V_t, we can verify that I_{det} increases practically linearly with I_{fwd}, as already shown in Fig. 2 (b) and Fig. 4.

Fig. 6 (a) Shows the same lasing information as described above, with slightly less resolution, in the form of P_{out} vs. V_t. There is no lasing below 7V of tuning voltage nor above 15V, as already concluded before. Fig. 6 (b) shows the direct relationship in between the detector electrical current and the VCSEL output power. Thus, the concept of integrated detector oblique to the optical cavity shows a monotonic behavior of I_{det} as function of output power, above threshold, at a given tuning voltage.

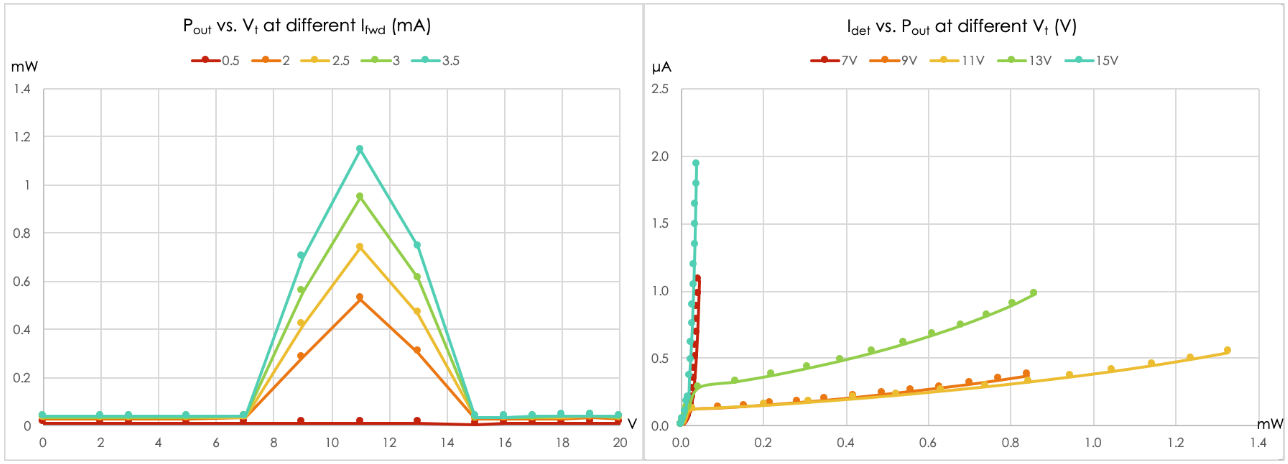

(a) (b)

Figure 6. (a) P_{out} (mW) vs. V_t (mA) at different I_{fwd}. This particular tunable VCSEL is only lasing in between 7V and 15V, with highest output power at V_t = 11V. (b) I_{det} (µA) vs. P_{out} (mW). I_{det} follows P_{out} monotonically above threshold at a given tuning voltage.

4. CONCLUSION

We report the design and manufacturing of a tunable VCSEL with an HCG MEMS mirror and an integrated detector oblique to the optical cavity for measuring output power without disturbing the laser cavity. The sacrificial layer defines a cavern around optical cavity which acts as a detector of scattered light coming from cavity. Light scattered at the interface semiconductor-air hits the cavern walls and modifies current I_{det}, which is monitored at the MEMS terminal. Any change in the VCSEL output power (P_{out}) is directly related to a change on I_{det}, creating a direct relationship of I_{det} vs P_{out}. To the best of our knowledge, there is no previous report of a VCSEL with integrated oblique intracavity detector.

ACKNOWLEDGEMENT

We would like to acknowledge Dr. Ghulam Hasnain for the always insightful analysis and discussions.

REFERENCES

[1] T. Taimre, M. Nikolić, K. Bertling, Y. L. Lim, T. Bosch, and A. D. Rakić, “Laser feedback interferometry: a tutorial on the self-mixing effect for coherent sensing,” *Adv. Opt. Photon.*, vol. 7, no. 3, p. 570, Sep. 2015, doi: 10.1364/AOP.7.000570.

[2] Bardinal, V. et al., "Integrated photodetection in VCSELs," Proceedings of 2005 7th International Conference Transparent Optical Networks, 2005., 2005, pp. 120-125 Vol. 2, https://doi.org/10.1109/ICTON.2005.1506113 .

[3] Lebby, M. S. et al., "VCSEL devices and packaging," Proc. SPIE 3289, Micro-Optics Integration and Assemblies, (20 April 1998); https://doi.org/10.1117/12.305470.

[4] Hasnain, G., Tai, K., Wang, Y. H., Wynn, J. D., Choquette, K. D., Weir, B. E., Cho, A. Y., “Monolithic integration of photodetector with vertical cavity surface emitting laser”. Electronics Letters, 27(18), 1630, 1991, https://doi.org/10.1049/el:19911019

[5] Lim, S. F., Lascola, K. M., Wupen Yuen, & Chang-Hasnain, C. J., “Optimization of VCSEL with an integrated resonant photodetector”. Conference Digest. ISLC 1998 NARA. 1998 IEEE 16th International Semiconductor Laser Conference, https://doi.org/10.1109/islc.1998.734157 .
[6] Steinle, G., Wolf, H., “VCSEL with monolithically integrated photodetector”, U.S. patent number 203/02132A1, Publication date Jan, 30th, 2003.
[7] Grabherr, M., Gerlach, P., King, R., Jaeger, R. (2009). Integrated photodiodes complement the VCSEL platform. Proceedings of SPIE - The International Society for Optical Engineering. 7229. https://doi.org/10.1117/12.808847 .
[8] Moench, H. et al., "ViP-VCSEL with integrated photodiode and new applications," Proc. SPIE 12020, Vertical-Cavity Surface-Emitting Lasers XXVI, 1202006 (2 March 2022); https://doi.org/10.1117/12.2607345.
[9] Chang-Hasnain, C. J., “Tunable VCSEL,” *IEEE J. Select. Topics Quantum Electron*, vol. 6, no. 6, pp. 978–987, 2000.
[10] Huang, M. C. Y. et al., “Demonstration of piezoelectric actuated GaAs-based MEMS tunable VCSEL,” *IEEE Photon. Technol. Lett.*, vol. 18, no. 10, pp. 1197–1199, May 2006, doi: 10.1109/LPT.2006.873923.
[11] Gierl, C. *et al.*, “Surface micromachined tunable 1.55 µm-VCSEL with 102 nm continuous single-mode tuning,” *Opt. Express*, vol. 19, no. 18, p. 17336, Aug. 2011, doi: 10.1364/OE.19.017336.
[12] Li, K., Chase, C., Qiao, P. and Chang-Hasnain, C. J., “Widely tunable 1060-nm VCSEL with high-contrast grating mirror,” *Optics Express*, vol. 25, no. 10, p. 11844, May 2017, doi: 10.1364/OE.25.011844.
[13] Ellafi, D. et al., "MEMs-HCG VCSELs for emerging sensing and datacom applications," Proc. SPIE 11300, Vertical-Cavity Surface-Emitting Lasers XXIV, 113000R (3 March 2020); https://doi.org/10.1117/12.2547396.